Time-resolved luminescence of perturbed biosystems: Stochastic models and perturbation measures

B. Kochel

Department of Toxicology, Medical Academy of Wroclaw, 57/59 Traugutta St., PL-50417 Wroclaw (Poland)

Abstract. Measures of biosystem perturbation using a cybernetic approach based on stochastic models of photon emission processes are presented, and compared with classical measures. Perturbation phenomena reflected in non-stationary emission processes are represented by means of filtering theory.
Key words. Biosystems; linear filters; perturbation measures; photon emission; stochastic models.

Introduction

Photon emission from various native living organisms, as well as from some of their subsystems, can be considered to be a stationary uncorrelated stochastic process if it is analyzed as a time-resolved phenomenon[15, 16, 24]. The stationary character of these processes seems to be easy to explain on a basis of the homeostasis of biosystems; according to this principle, a biosystem maintains its internal process(es) in a steady state. This means that light-producing reactants and/or reactions are kept at constant stationary levels.

However, for the following reasons, and perhaps others, the notion of homeostasis in its classical meaning[6, 14] cannot be used as a general explanation of the stationary character of the process. Firstly, apart from some simple model reactions, the light-producing processes are unstable, complex multistage processes with parameters that vary both within and between the stages. Secondly, contemporary measuring techniques allow one to register only the total emission from a biosystem, disregarding possible different contributions of different active subsystems; in consequence, during the measurement a variety of different (in general: non-stationary, correlated) processes is transformed into a single stationary, uncorrelated process, i.e. a white noise.

In order to take into account non-stationary processes, e.g. periodic ones, the notion of homeoresis[31] should be employed. In conclusion, the stationary nature of photon emission may be considered at most as a resultant characteristic of an entire biosystem or its large subsystems; the same restriction applies to the notion of homeostasis. There are, however, some native biosystems in which photon emission shows non-stationary behaviour; it may be periodic[8, 26, 27] or have other characteristics[1, 7, 11, 19, 32]. In such cases, the notions of the homeostasis of biosystems and of the stationarity of photon emission are useless, even as resultant characteristics of biosystems, and cannot serve as starting points for constructing measurements of perturbation of biosystems founded on photon emission processes.

Photon emission from perturbed biosystems: Stochastic models

External indications of perturbations of biohomeostasis or biohomeoresis, consisting of changes in levels or in fluxes, respectively, of substances which are essential for maintaining the internal structure and functions of a biosystem, can be observed as a deviation of photon emission from either stationary uncorrelated processes or from certain non-stationary (e.g. seasonal[8, 26, 27], or other[19]) processes in a native biosystem.

The deviation is, in general, represented by the appearance of a non-stationary correlated process. Such a process, no matter what perturbers and biosystems are considered, consists of two stages: ascending and descending. Examples of this phenomenon can be found for plants[3, 16, 29], microorganisms[17, 26, 27], small animals[24, 25], and subsystems of the human organism[1, 7, 11–13, 19, 20, 23, 32]. This phenomenon is illustrated in figure 1. Stability of this form over a variety of biosystems and their perturbers suggests that it should not be considered as a chemical side-reaction but as an essential feature of perturbed behaviour, and in consequence it calls for comprehensive analyses, including a cybernetic one. Both of the stages can be adequately modelled as autoregressive-integrated moving average (ARIMA) processes using the methods described by Box and Jenkins[4].

General form of the ARIMA(p, d, q) model:

$$\varphi(B)(1 - B)^d n(t) = \vartheta(B)\, a(t), \quad (1)$$

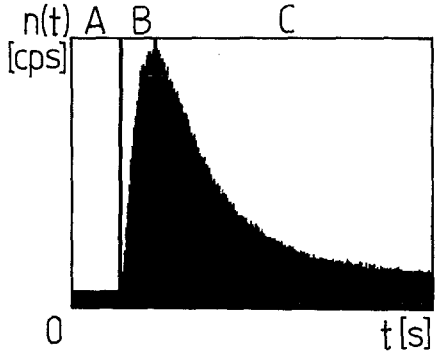

Figure 1. An example of the photon emission process generated by native yeast (A) and yeast perturbed with 8% formaldehyde (B, C). The process A is stationary, uncorrelated and Gaussian; the non-stationary process B–C is composed of an ascending stage (B) followed by a descending (quasirelaxation) one (C). The ascending stage is described by an ARIMA(1, 2, 1) stochastic model, whereas the descending one is described by an IMA(0, 1, 1) model[17]. It is important to note that the presented behaviour is of general importance for many different biosystems and perturbers.

where $\varphi(B) = 1 - \sum_{\tau=1}^{p} \varphi_\tau B^\tau$ and $\vartheta(B) = 1 - \sum_{\tau=1}^{q} \vartheta_\tau B^\tau$ are the pth- and qth-order autoregressive and moving average operators, $(1 - B)^d$ and B are the dth-order difference and back shift operators, transforms a white noise process $\{a(t)\}$ into a stationary/non-stationary correlated/uncorrelated process $\{n(t)\}$. $n(t)$ denotes the number of photoelectrons registered during the time interval $(t, t + \Delta t)$, where Δt is the counting time. The photon-counting and photon-number statistics differ from one another only by a scale change given by the photoefficiency of the detector[22], therefore $n(t)$ and $\{n(t)\}$ can be viewed, respectively, as the number of emitted photons and the photon-emission time series taken by homomorphism.

Eq. 1 takes the form of the IMA(0, 1, 1) or ARIMA(1, 2, 1) models for all non-stationary photon emissions from perturbed biosystems that have been analyzed by the author up to now. Perturber-induced ascending stages of these photon emission processes are described by the ARIMA(1, 2, 1) model with various parameters, whereas the descending stages are mostly modelled as IMA(0, 1, 1) processes[16-19,24]; ARIMA(1, 2, 1) was found to be appropriate only for one instance as a model of the descending stage[24]. Those models were determined using the correlation and Fourier spectral analyses applied to photon-emission processes.

The integrated moving average process IMA(0, 1, 1):

$$(1 - B)\, n(t) = (1 - \vartheta B)\, a(t) \tag{2}$$

is parametrised by ϑ fulfilling the reversibility condition $|\vartheta| < 1$ and the variance of white noise $\sigma^2_{a(t)} = \sigma^2_{(1-B)n(t)}/(1 + \vartheta^2)$, where $\sigma^2_{(1-B)n(t)}$ is the variance of difference process $\{(1 - B)\, n(t)\}$. The ϑ value is determined by minimizing the conditional sum of residual squares

$$S(\vartheta \mid \hat{a}(0) = 0) = \sum_{\tau} [(1 - B)\, n(t) - \vartheta \hat{a}(t-1)]^2 \ ^{16,19,24}.$$

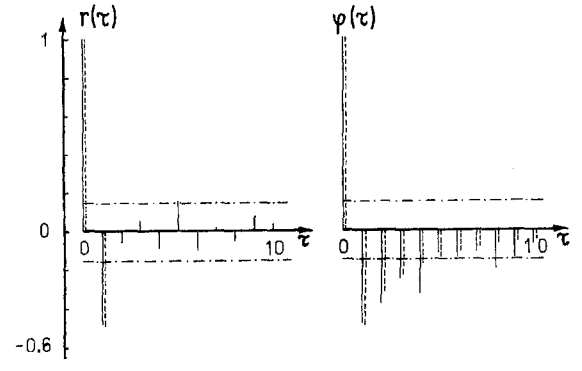

Figure 2. Common and partial correlation functions $r(\tau)$ and $\varphi(\tau, \tau)$ of the descending stage of the IMA(0, 1, 1) non-stationary photon emission process, generated by green wheat leaves perturbed by the temperature 320 K. Theoretical values (dashed bars) of the MA(1) model have been compared with empirical ones (solid bars) for the difference process $\{(1 - B)\, n(t)\}$. The 95% confidence intervals for the correlation fluctuations of a white noise are plotted. Parameters of the model are $\vartheta = 0.82 \pm 0.04$, and $\sigma^2_{a(t)} = 329.49\,(\text{cps})^2$[16].

Common and partial autocorrelation functions corresponding to the 1st-order moving average model MA(1) of $\{(1 - B)\, n(t)\}$, having the forms:

$$r(\tau) = \begin{cases} -\vartheta/(1+\vartheta^2), & \tau = 1 \\ 0 \quad\quad\quad\quad , & \tau > 0 \end{cases} \tag{3}$$

$$\varphi(\tau, \tau) = \frac{-\vartheta^\tau(1-\vartheta^2)}{1-\vartheta^{2(\tau+1)}}, \quad \tau = 1, 2, \ldots \tag{4}$$

where τ is a time lag, are shown in figure 2 for the descending stage of the IMA(0, 1, 1) process generated by wheat leaves perturbed by high temperature[16].

Power spectral density function $g(f)$ of the same moving average process is as follows:

$$g(f) = \frac{2}{N-2} \frac{1 + \vartheta^2 - 2\vartheta \cos 2\pi f}{1 + \vartheta^2}, \quad f \in [0, 0.5] \tag{5}$$

where $\sum_f g(f) = 1$. An example is shown in figure 3.

Non-stationarity of a photon emission process $\{n(t)\}$ calls for finding such a dth-degree difference process $\{(1 - B)^d\, n(t)\}$ which might be considered to be stationary by correlation or spectral analyses. An example of the application of the integrated spectral density function $C(f') = \sum_{f=0}^{f'} g(f)$ (cumulative periodogram) to the 1st-degree difference process for perturbed wheat leaves is presented in figure 4. By comparison with figure 5 one can verify the adequacy of the accepted model IMA(0, 1, 1). This adequacy can also be tested by investigation if the $C(f)$ function of the residual series $\{\hat{a}(t)\}$ does not differ from that of white noise $\{a(t)\}$; it is illustrated in figure 6. The autoregressive-integrated moving average process ARIMA(1, 2, 1):

$$(1 - \varphi B)(1 - B)^2\, n(t) = (1 - \vartheta B)\, a(t) \tag{6}$$

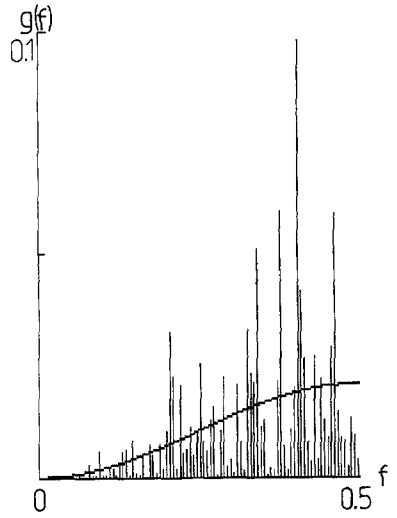

Figure 3. Theoretical (continuous line) and empirical (bars) power spectral density functions $g(f)$ for the descending stage of the non-stationary photon emission from perturbed green wheat leaves at 320 K[16]. Employed model is the same as in fig. 2.

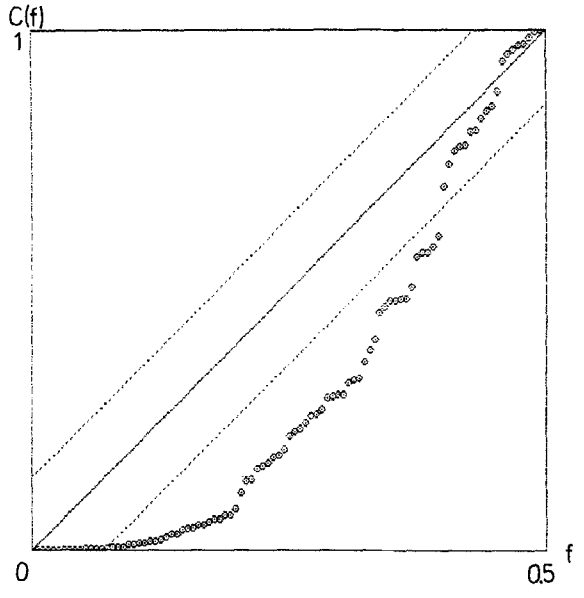

Figure 4. Empirical integrated spectral density function C(f) of the difference process $\{(1 - B)\, n(t)\}$ for the emission described in figs 2 and 3. The C(f) function significantly ($p < 0.05$) deviates from the analogous function of a stationary uncorrelated Gaussian process. The 95% confidence intervals (dotted lines) resulting from a Smirnov-Kolmogorov test are plotted.

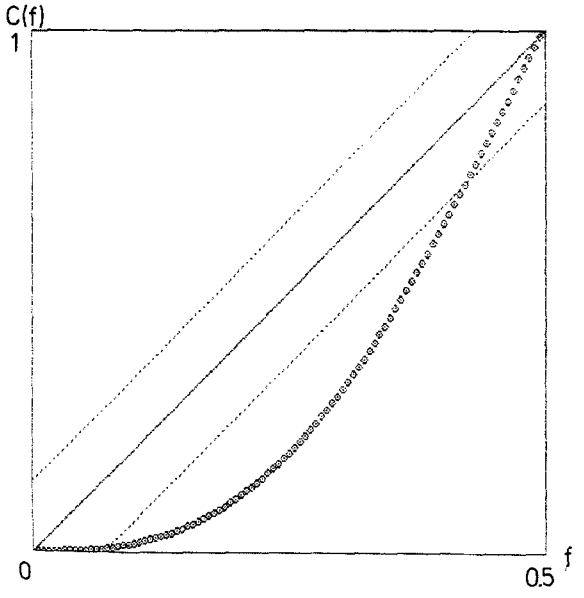

Figure 5. Theoretical integrated spectral density function C(f) of the difference process from fig. 4, modelled as the MA(1) process with $\vartheta = 0.82$.

is parametrised by $\varphi(|\varphi| < 1)$, $\vartheta(|\vartheta| < 1)$ and variance $\sigma^2_{a(t)} = \sigma^2_{(1-B)^2 n(t)}(1 - \varphi^2)/(1 + \vartheta^2 - 2\varphi\vartheta)$, where $\sigma^2_{(1-B)^2 n(t)}$ is the variance of $\{(1 - B)^2 n(t)\}$ process. The φ and ϑ parameters result from minimizing the sum $S(\varphi, \vartheta | \hat{a}(0) = 0) = \sum_\tau \{(1 - B)^2 [n(t) - \varphi n(t - 1)] + \vartheta \hat{a}(t - 1)\}^2$ [24].

The common correlation function $r(\tau)$ corresponding to the ARIMA(1, 1) model of the 2nd-degree difference process $\{(1 - B)^2 n(t)\}$ takes the form [24]:

$$r(\tau) = \frac{(1 - \varphi\vartheta)(\varphi - \vartheta)\varphi^{\tau - 1}}{1 + \vartheta^2 - 2\varphi\vartheta}, \quad \tau = 1, 2, \ldots \tag{7}$$

and a power spectral density function $g(f)$ is as follows [23]:

$$g(f) = \frac{2}{N-3} \cdot \frac{(1 - \vartheta^2)(1 + \vartheta^2 - 2\varphi\vartheta\cos 2\pi f)}{(1 + \vartheta^2 - 2\varphi\vartheta)(1 + \varphi^2 - 2\varphi\vartheta\cos 2\pi f)}, \quad f \in [0, 0.5] \tag{8}$$

where $\sum_f g(f) = 1$.

The idea of representing the temporal behaviour of non-stationary photon emissions by linear stochastic models has resulted in: 1) the finding of a simple and computationally effective method for describing perturbations of various biosystems in a few common forms: IMA(0, 1, 1) and ARIMA(1, 2, 1); 2) the finding that essential information about perturbation, owing to the condition of repeatability, is contained in the descending stage of the non-stationary process [19]; 3) the possibility of constructing non-local perturbation measurements, such as the notions of memory [17, 18] and perturbation coefficient [19].

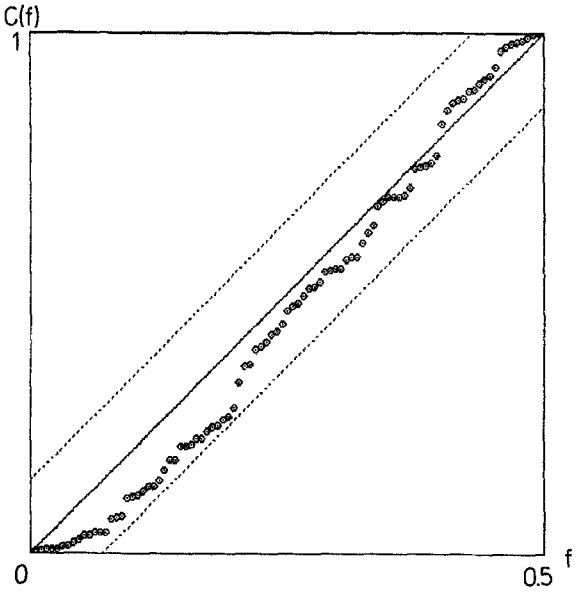

Figure 6. Integrated spectral density function C(f) of the residuals from fitting the descending stage of the $\{n(t)\}$ process with the IMA(0, 1, 1) model. The example of green wheat leaves at 320 K is still demonstrated. One can see that the C(f) function does not differ significantly (at $p < 0.05$) from a white noise; this testifies to the adequacy of the IMA(0, 1, 1) model.

Memory of a biosystem

In rational continuum mechanics [28] and thermodynamics [10], a notion of memory function has existed for more

than thirty years[9]. Searching for the explicit form of a temporal dependence of the states of a system was a motive for introducing the notion of an obliviator[9] and then of memory. The same motive, and a psychological commonsense-conjecture that intense experiences will relegate the past into oblivion was a starting point for considering the time structure of non-stationary photon emission processes, induced by perturbers acting as obliviators[16-18].

The internal temporal dependence of photon emissions in their descending (quasirelaxation) stage can be obtained from the stochastic models IMA(0, 1, 1) (2) and ARIMA(1, 2, 1) (6) by using the difference operator $\pi(B) = 1 - \sum_{\tau=1}^{\infty} \pi_\tau B^\tau$ which transforms $\{n(t)\}$ into $\{a(t)\}$, i.e. $\pi(B)\, n(t) = a(t)$[16-18].

For the IMA(0, 1, 1) and ARIMA(1, 2, 1) models $\pi(B)$ takes, respectively, the forms[17,18]:

$$\pi(B) = \begin{cases} (1-\vartheta B)^{-1}(1-B) & , \text{IMA}(0,1,1) \\ (1-\vartheta B)^{-1}(1-\varphi B)^2(1-B)^2, & \text{ARIMA}(1,2,1) \end{cases} \tag{9}$$

In consequence the π_τ weights of the IMA(0, 1, 1) process are described as follows:

$$\pi_\tau = (1-\vartheta)\vartheta^{\tau-1}, \quad \tau = 1, 2, \ldots \tag{10}$$

and the present state n(t) of this process can be expressed by its previous states $n(t-\tau)$ as a linear combination:

$$n(t) = a(t) + \sum_{\tau=1}^{\infty} \pi_\tau n(t-\tau). \tag{11}$$

Since $\sum_{\tau=1}^{\infty} \pi_\tau = 1$ all the states $n(t-\tau)$ up to $-\infty$ entirely determine the current state n(t). However, their contributions to n(t) depend on the ϑ parameter and the time lag τ (see the function $\pi = \pi(\vartheta)$ in fig. 7, and the functions $\pi = \pi(\tau)$ at fixed $\vartheta = 0.55$ and 0.09 in figs 8 and 9). The π_τ weights of the ARIMA(1, 2, 1) process having the form[17,18]:

$$\pi_\tau = \begin{cases} -\vartheta + 2 + \varphi & , \tau = 1 \\ -\vartheta^\tau + (2+\varphi)\vartheta - (1+2\varphi) & , \tau = 2 \\ -\vartheta^\tau + (2+\varphi)\vartheta^{\tau-1} - (1+2\varphi)\vartheta^{\tau-2} + \varphi\vartheta^{\tau-3} & , \tau \geqq 3 \end{cases} \tag{12}$$

are shown in figure 10.

Eq. 11, holding true for both models being considered here, suggests the possibility of interpreting the π_τ weights in terms of probability. Those weights, however, do not satisfy the condition $\pi_\tau \in [0, 1]$; this can be seen in figures 7 and 10. In order to make such an interpretation possible the normalised weights π_τ^*[17,18] must be considered:

$$\pi_\tau^* = \frac{|\pi_\tau|}{\|\pi_\tau\|} \tag{13}$$

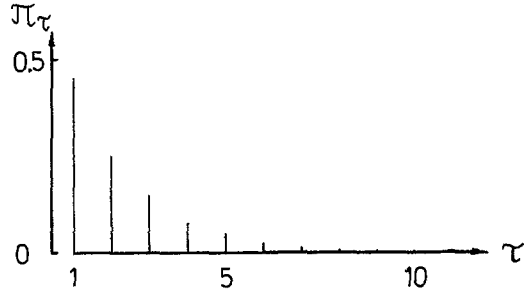

Figure 8. π_τ weight of the IMA(0, 1, 1) model as a function of time lag τ. An example of the descending stage of the photon emission from yeast perturbed by the 0.031% formaldehyde[17]. The π_τ values have been calculated at $\vartheta = 0.55$.

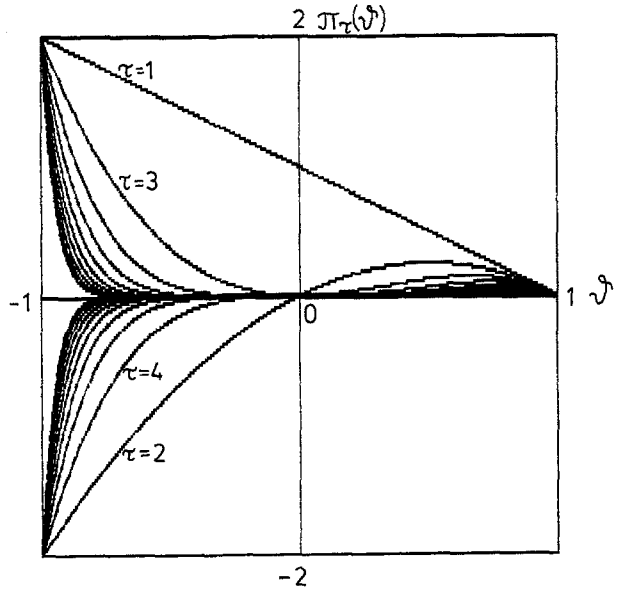

Figure 7. A set of the π_τ weights ($\tau = 1, 2, \ldots, 20$) of the IMA(0, 1, 1) process. The weights are shown as functions $\pi_\tau(\vartheta)$ of the model parameter ϑ.

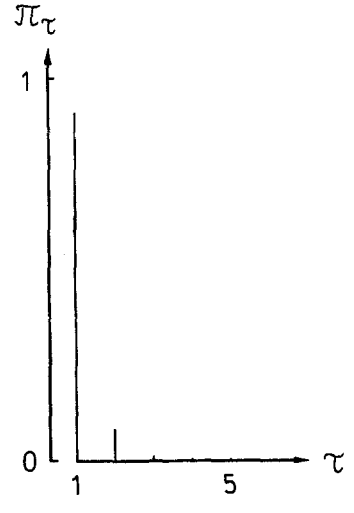

Figure 9. π_τ weight of the IMA(0, 1, 1) model as a function $\pi = \pi(\tau)$. The same example as in fig. 8 but at a much higher concentration of the perturber: 2%. The ϑ parameter is 0.09. In comparison to fig. 8 these π_τ values vanish considerably more rapidly.

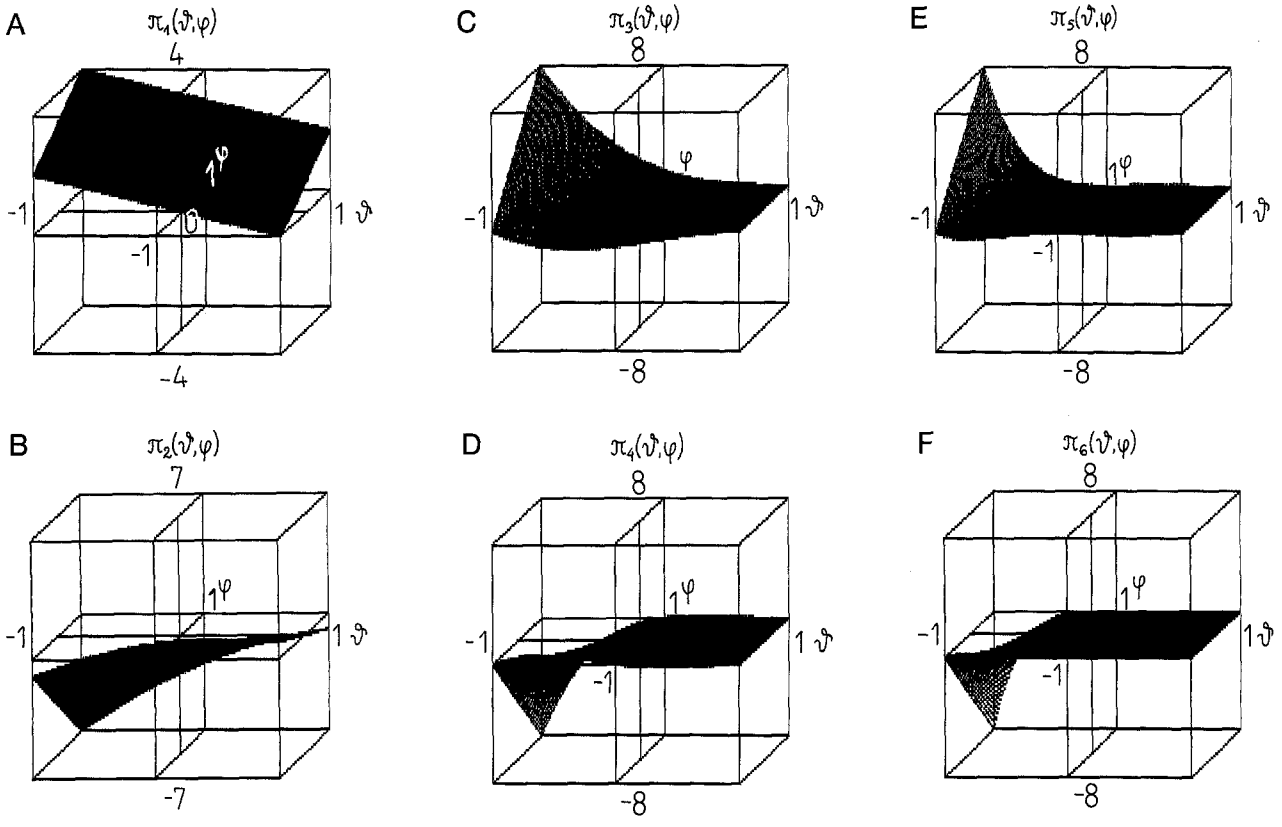

Figure 10. The first six $\pi_\tau(\vartheta, \varphi)$ weights of the ARIMA(1, 2, 1) model as functions of ϑ and φ. The odd weights ($\tau = 1, 3, 5$) show a different behaviour from the even ones ($\tau = 2, 4, 6$)[17,18].

where $\|\pi_\tau\| = \sum_{\tau=1}^{\infty} |\pi_\tau|$ is a norm of the weight function π. This norm as a limit of a function series is a function. In the case of the IMA(0, 1, 1) process the norm $\|\pi_\tau\|$ takes one of the following functions[17,18]:

$$\|\pi_\tau\| = \begin{cases} 1 & \text{for } \vartheta \in [0, 1) \\ \dfrac{1-\vartheta}{1+\vartheta} & \text{for } \vartheta \in (-1, 0] \end{cases} \tag{14}$$

whereas for the ARIMA(1, 2, 1) process it converges to one of the six following functions[17,18]:

$$\text{(A)} \quad \frac{-\vartheta + 4\varphi + 3}{\vartheta + 1} \qquad \text{for } \varphi \geqq \vartheta \text{ and } \vartheta \geqq 0,$$

$$\text{(B)} \quad 2\vartheta^2 - \vartheta(2\varphi + 4) + 4\varphi + 3 \quad \text{for } \varphi \geqq \vartheta \text{ and } \vartheta \geqq 0,$$

$$\text{(C)} \quad -2\vartheta + 2\varphi + 3 \qquad \text{for } \vartheta \geqq \varphi \geqq (\vartheta^2 - 2\vartheta + 1)/(\vartheta - 2) \text{ and } \vartheta \geqq 0,$$

$$\text{(D)} \quad 2[-\vartheta^2 + \vartheta(1 + \varphi) - \varphi] + 1 \qquad \text{for } \varphi \leqq (\vartheta^2 - 2\vartheta + 1)/(\vartheta - 2) \text{ and } \vartheta \geqq 0,$$

$$\text{(E)} \quad [-2\vartheta^2 + \vartheta(2\varphi + 3) - 2\varphi + 1]/(\vartheta + 1) \qquad \text{for } \varphi \leqq (\vartheta^2 - 2\vartheta + 1)/(\vartheta - 2) \text{ and } \vartheta \leqq 0. \tag{15}$$

The convergence areas $\|\pi_\tau\|$ of the ARIMA(1, 2, 1) process have been shown in figure 11.

The normalised weights π_τ^* of both models satisfy the probability conditions: $\pi_\tau^* \in (0, 1)$ and $\sum_{\tau=1}^{\infty} \pi_\tau^* = 1$, thus they can be interpreted as probabilities of influence of $n(t - \tau)$ states on $n(t)$. A function $\pi^*: \mathbb{N} \to \mathbb{R}_+$, where $\mathbb{N}$ and $\mathbb{R}_+$ denote the sets of the natural and positive real numbers, which maps $\tau \in \mathbb{N}$ to $\pi_\tau^* \in (0, 1)$, can be proposed as a memory function[17,18].

The memory function of the IMA(0, 1, 1) process is a monotonically decreasing function of τ at any $\vartheta \in (-1, 1) - \{0\}$, and $\lim_{\tau \to \infty} \pi_\tau^* = 0$. This means that the more distant the state $n(t - \tau)$ the weaker is its influence on $n(t)$, and infinitely distant states do not affect $n(t)$. In the case of the ARIMA(1, 2, 1) process the memory function is not in general a monotonic function of τ, although its values tend to zero when $\tau \to \infty$. It monotonically decreases for $\tau \to \infty$ if, and only if, the pair (φ, ϑ) takes values from M areas in figure 12. Otherwise the memory function is not a monotonic function of τ. It is interesting to compare this function to the function of Coleman and Noll[9]: the former is either monotonic or nonmonotonic, whereas the latter is only monotonic; however, both of them are fading with time. The assumption of monotonicity of the memory function does not

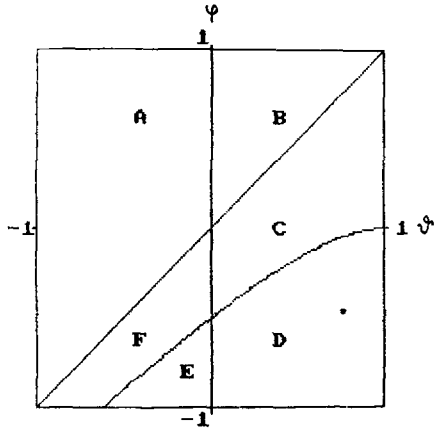

Figure 11. Convergence areas (A–F) of the infinite function series $\sum_\tau |\pi_\tau|$ of the ARIMA(1, 2, 1) model[17, 18]. Different series converge to one and the same function if their parameters (ϑ, φ) fall into the same convergence area. Lines $\vartheta = 0$, $\varphi = \vartheta$ and $\varphi = (\vartheta^2 - 2\vartheta + 1)/(\vartheta - 2)$ separete different convergence areas. Point (ϑ, φ) = (0.76, – 0.46) located in the D area represents the ARIMA(1, 2, 1) photon emission process (in its descending stage) generated by rose flowers perturbed by formaldehyde[24].

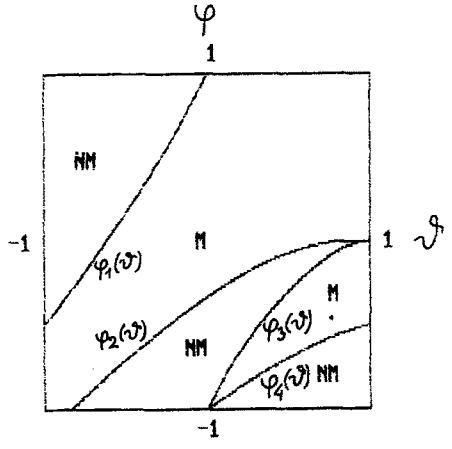

Figure 12. Areas of monotonic (M) and nonmonotonic (NM) behaviour of the normalised weights π_τ^* of the ARIMA(1, 2, 1) process[17, 18]. Normalised weights for rose flowers perturbed by formaldehyde are localized in the monotonic area.

seem to be justifiable, because of the occurrence of (quasi)-periodic processes (presented e.g. in refs 8, 26, 27) in biosystems; for such processes, e.g. for IMA(0, 1, 1) × IMA(0, 1, 1)$_s$[4], the memory function is a superposition of oscillations and exponentials.

In practice, owing to the fading of the memory function, its π_τ^* weights at a certain τ must be considered as insignificantly different from zero. The current value n(t) depends on the finite number of previous values n(t – τ). Mathematical formalization of that problem has been carried out in the following way[17, 18]. Let $H_t = \{n(t-\tau): \tau = 1, 2, \ldots\}$ be an ordered set of all states n(t – τ) which precede n(t); the set H_t composes the whole history of the process {n(t)} for any given moment t. Let J be a time moment which splits the process history H_t into two subsets: $\{n(t-\tau): \tau = 1, 2, \ldots, J\}$ and $\{n(t-\tau): \tau = J+1, J+2, \ldots\}$, where the former is assumed to influence the current state n(t) with a certain probability δ ($\delta \in [0, 1]$) called a determination level[17, 18]. At $\delta < 1$ the history is finite, i.e. the memory is extended up to a time moment J. This means that the memory function π_τ^* has been cut off to the function $\pi_C^*: \mathbb{N} \supset \mathbb{X} \to \mathbb{R}_+$ which maps a finite subset X of the natural numbers τ to the open interval $(0, 1) \supset \mathbb{R}_+$. A map $M: \pi_C^*(\tau) \to \sum_{\tau=1}^{J} \pi_\tau^*$ which associates, at a given δ, to each cut memory function $\pi_C^*(\tau)$ the number $M[\pi_C^*(\tau)] = \sum_{\tau=1}^{J} \pi_\tau^*$, defines the memory functional of process {n(t)}.

The notion of the memory functional can be useful for determining the memory time $T_M = f(J)\,\Delta t$ of a process {n(t)}[17, 18], where Δt_c is a counting time, and f(J) = J or 2J – 1, if the dead time of recorder Δt_d is zero, or respectively, $\Delta t_d = \Delta t_c$. The hypothesis that the stronger the perturbation the lower the memory time T_M, and vice versa, has been verified for the IMA(0, 1, 1) photon emission processes generated by perturbed yeast[17].

For the IMA(0, 1, 1) process the memory functional[17]:

$$M[\pi_C^*(\tau)] = \sum_{\tau=1}^{J} \pi_\tau^* = \frac{1-\vartheta}{\vartheta} \sum_{\tau=1}^{J} \vartheta^\tau = 1 - \vartheta^J, \quad (J \geq 1) \tag{16}$$

leads, at a determination level δ and $\Delta t_d = 0$ to the memory time[17].

$$T_M = \frac{\ln(1-\delta)}{\ln \vartheta} \Delta t_c \tag{17a}$$

or

$$T_M = \left(\frac{2\ln(1-\delta)}{\ln \vartheta} - 1\right) \Delta t_c, \quad \text{if } \Delta t_d = \Delta t_c. \tag{17b}$$

Results of the experimental verification of the above hypothesis have been demonstrated in figure 13.

T_M (Eq. 17) is a monotonically increasing function of ϑ at any $\vartheta \in (0, 1)$; consequently, in the absence of perturba-

Perturber	Concentration [mM]	$\vartheta \pm SD(\vartheta)$	$T_M^* \pm SD(T_M)$** [s]	PC ± SD(PC) [%]	CPC [%]
DMSO	21.0	0.80 ± 0.03	4.03 ± 6.9	28.6 ± 4.7	21.6
o-xylene	1.0	0.72 ± 0.04	27.0 ± 4.7	41.8 ± 6.7	40.1
p-xylene	1.0	0.68 ± 0.04	22.9 ± 3.6	45.7 ± 6.9	6.9
Toluene	2.5	0.60 ± 0.05	17.0 ± 2.4	57.1 ± 7.5	24.1
Benzene	5.0	0.59 ± 0.05	16.5 ± 2.2	58.6 ± 7.6	35.3
Phenol	0.2	0.59 ± 0.05	16.5 ± 2.2	58.6 ± 7.6	49.8

* At $\delta = 0.99$, $\Delta t_c = \Delta t_d = 1$; see Eq. 17b. ** $SD(T_M) = -2SD(\vartheta)\frac{\ln(1-\delta)}{\vartheta \ln^2 \vartheta} \Delta t_c$.

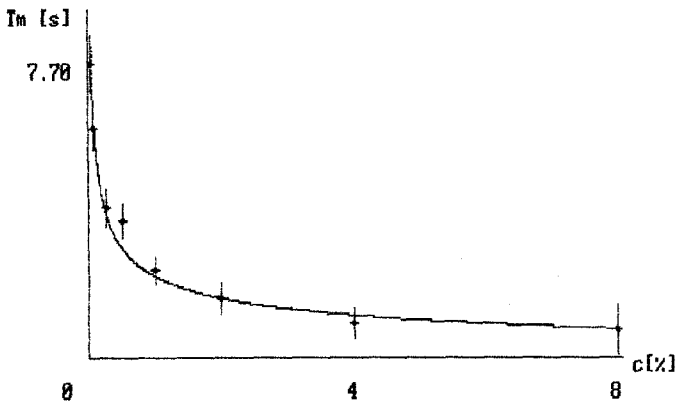

Figure 13. Memory time T_M of yeast perturbed by formaldehyde as a function of formaldehyde concentration c[17]. Power regression $T_M = 2.46\,c^{-0.35}$ fits the empirical values with correlation coefficient: -0.99. Memory time values $T_M = \ln(1-\delta)/\ln\vartheta$ at $\delta = 0.99$ ($\Delta t_c = 1$ s and $\Delta t_d = 0$) are accompanied by their standard deviations $SD(T_M) = -\ln(1-\delta)/(\vartheta \ln^2\vartheta)\,((1-\vartheta^2)/(N-2))^{1/2}$. Descending stages of the photon emission processes occurring at all used concentrations have been modelled as IMA(0, 1, 1) processes. One can see that the greater the perturbation (perturber concentration), the shorter the memory time.

tion the parameter ϑ tends to 1, and T_M tends to infinity. Simultaneously, when $\vartheta \to 1$ then the IMA(0, 1, 1) process converges into a white noise (see Eq. 2) corresponding to an unperturbed biosystem. N.B. the memory of a white noise is extended over whole the infinite past; however, with zero weights. One can see from power regression in figure 13 that $T_M \to \infty$ when $c \to 0$.

Analogously, the memory functional and memory time for the ARIMA(1, 2, 1) process take, respectively, the forms[17]:

$$M[\pi_c^*(\tau)] = \sum_{\tau=1}^{J} \pi_\tau^* = 1 - \frac{\vartheta^{J-2}}{2 + [-\vartheta^2 + \vartheta(1+\varphi) - \varphi]^{-1}} \quad (J \geqq 2) \tag{18}$$

$$T_M = \frac{2 + \ln\{(1-\delta)[2 + (-\vartheta^2 + \vartheta(1+\varphi) - \varphi)^{-1}]\}}{\ln\vartheta} \cdot \Delta t_c \quad (\Delta t_d = 0) \tag{19}$$

Memory time can be employed as a perturbation measure; this measure, as based on the entire quasirelaxation process, is non-local and unambiguous, in contrast to other local and ambiguous measures which are being used now in studies of biochemiluminescence[1, 20, 25]; however, this measure is burdened with some inconveniences resulting from the fact that it is inversely proportional to perturbation, and unnormed.

The perturbation phenomenon as a filtering process

In the cases when photon emission processes from native (unperturbed) biosystems are stationary, uncorrelated ones, the effects of perturbers leading to non-stationarity can be evaluated by means of filtering theory[2, 4]. If the linear stochastic models of photon emission processes are employed, then the linear filters whose input and output are, respectively, stationary uncorrelated $\{a(t)\}$ and non-stationary $\{n(t)\}$ processes should be applied.

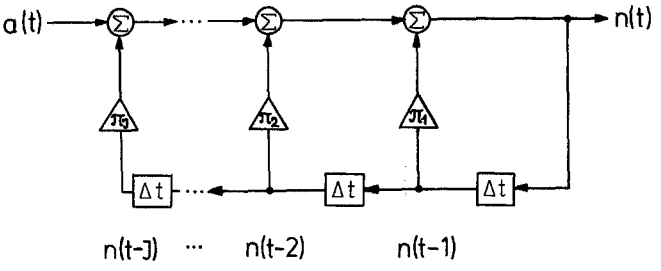

Figure 14. Recursive filter representing a perturbed biosystem. An input (stationary uncorrelated) process $\{a(t)\}$ corresponding to an unperturbed biosystem is transformed into an output (non-stationary correlated) process $\{n(t)\}$ corresponding to a perturbed biosystem. There exists a delay line in the filter, making possible a regression of the current system's state on its previous states. Time quantities t and τ ($\tau = 1, 2, \ldots, J$) are expressed in the counting time units Δt.

By using the transfer function $\Psi(B) = 1 + \sum_{\tau=1}^{\infty} \Psi_\tau B^\tau$, a perturbed biosystem, the $\{n(t)\}$ process of which is modelled by IMA(0, 1, 1), can be represented as an unstable linear filter having the fixed weights

$$\Psi_\tau = 1 - \vartheta; \tag{20}$$

$\lim_{\tau \to \infty} \Psi_\tau \neq 0$ results in instability of the filter[18].

By analogy, the transfer function weights Ψ_τ of the filter transforming $\{a(t)\}$ into the ARIMA(1, 2, 1) process can be written in the form[18]:

$$\psi_\tau = \begin{cases} 2 + \varphi - \vartheta, & \tau = 1 \\ (2+\varphi)\psi_1 - (1+2\varphi), & \tau = 2 \\ (2+\varphi)\psi_{\tau-1} - (1+2\varphi)\psi_{\tau-2} + \varphi\psi_{\tau-3}, & \tau \geqq 3. \end{cases} \tag{21}$$

This filter is also unstable.

It is possible to represent the effects of perturbation differently by linear filtering, namely through recursive filters. In contrast to nonrecursive filters with weights (20) and (21), the current output value n(t) can be described by previous output values $n(t-\tau)$ instead of $a(t-\tau)$. Such a recursive filter is depicted in figure 14, where $\sum$, Δ and $\square$ denote summation, multiplication and time delay, respectively.

With reference to the introductory remarks it should be emphasized that in the majority of native emissions from large complex biosystems one encounters a superposition of many different radiations. Therefore the resulting process is chaotic, and can be described by Pascal or Gauss distributions, even if some of its components were coherent[21, 22]. It is a simple inference from the facts that: 1) a Pascal distribution:

$$p(n) = \binom{M+n-1}{n} \rho^M (1-\rho)^n, \tag{22}$$

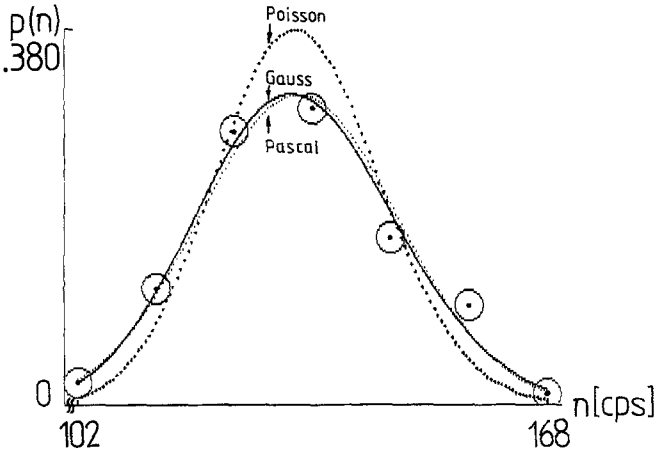

Figure 15. Poisson, Gauss and Pascal probability density functions p(n) of the stationary uncorrelated photon emission process, generated by unperturbed wheat leaves (*Triticum aestivum*) at 308 K. Maximal p(n) values of the Poisson, Gauss, Pascal and empirical distributions are 0.380, 0.314, 0.308 and 0.299, respectively. Mean value and variance equal to $\langle n \rangle = 133.0 \pm 1.0$ cps and $\sigma^2_{n(t)} = 177.4\,(\text{cps})^2$. According to a chi-square test showing that the critical value $\chi^2_{0.05} = 9.488$, the Poisson distribution with $\chi^2 = 23.647$ should be rejected. The Pascal ($\chi^2 = 3.209$) and Gauss ($\chi^2 = 3.851$) distributions are acceptable. For comparison see e.g. ref. 16.

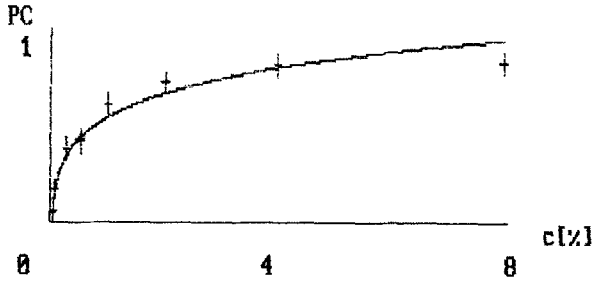

Figure 16. Perturbation coefficient $PC = 1 - |\vartheta|$ of yeast vs formaldehyde concentration c. Direct proportionality between the perturber concentration and its effect is maintained using this definition. However, the range of application of the definition is limited to the cases when a reference process is stationary and uncorrelated (see input process {a(t)} in fig. 14).

where M is the number of modes, n is the number of registered photons (n = 0, 1, 2, ... 0), $\langle n \rangle$ is a mean value of variable n, $\rho \equiv \frac{M}{M + \langle n \rangle}$, and $\rho \in (0, 1)$, is the M-fold convolution of the geometrical distributions:

$$p(n) = \rho(1 - \rho)^n = \frac{\langle n \rangle^n}{(1 + \langle n \rangle)^{n+1}}, \tag{23}$$

and that 2) a Pascal distribution tends to a Gaussian one if $M \to \infty$ at $\rho = \text{const}$. It should be added, however, that if $\rho \to 1$ at $\langle n \rangle = \text{const}$, then the limiting distribution of a Pascal one is a Poisson distribution:

$$p(n) = \frac{\langle n \rangle^n}{n!} e^{-\langle n \rangle}. \tag{24}$$

An experimental example of the verification of Pascal, Gauss and Poisson photon-counting distributions for an unperturbed biosystem is shown in figure 15. Lack of correlation, and a Gauss distribution, lead to white noise.

Non-local perturbation measures

Except for a few articles cited her, there have been no others relating to stochastic models in the field of biochemiluminescence. All the known attempts that have used time domain analysis have employed, in the end, exponential, hyperbolic and other regressions to describe only the kinetics of chemical reactions. In particular, this has resulted in a scantiness of perturbation measures. Those measures are founded on either ambiguous quantities (the integral luminescence/the integral of total counts/the total number of photons), or local characteristics (the maximal value/the value of the peak, the nodal time/the time to reach the peak)[1, 20, 25].

The memory time T_M has been announced to be a non-local perturbation measure because it is founded on the parameters of stochastic models describing perturbed biosystems. Another, much simpler measure can be defined, in the instance of the IMA(0, 1, 1) process, by the equation

$$PC \equiv 1 - |\vartheta|, \tag{25}$$

where PC is a perturbation coefficient ($PC \in [0, 1]$). PC = 0 if there is no perturbation ($\vartheta = 1$) in a biosystem; this means that {n(t)} = {a(t)}. For $\vartheta = 0$ there exists maximal perturbation PC = 1 (100%). One can observe in figure 16 that the biosystem is almost entirely perturbed at c = 8% ($\vartheta = 0.02$, PC = 0.98); this is confirmed by a plateau in PC = PC(c) around the concentration 8%.

The situation is more complicated when unperturbed biosystems emit non-stationary photon fluxes. Then the non-stationary emissions from perturbed biosystems cannot be referred to stationary uncorrelated emissions. Such a situation occurs in human neutrophils[19]; it is shown in figure 17.

It is important to notice that the form of the non-stationary emissions from perturbed phagocytosing neutrophils is common for perturbers as different as heavy metals[12], acidity[32], azides[11], fluorides[7], benzoates[7], prostaglandins[7], superoxide dismutase[11], and polychlorobiphenyl[13].

Consider a collection of processes from figure 17. Any perturbed phagocytosis process $\{n_{pert}(t)\}$ takes place in the space between a native phagocytosis process $\{n_{nat}(t)\}$ and the abscissa Ot (where a process in totally perturbed phagocytosing neutrophils is located, together with a background white noise). Let a resulting process $\{n_r(t)\}$ be defined by the following comparison of $\{n_{pert}(t)\}$ to $\{n_{nat}(t)\}$[19]:

$$\{n_r(t)\} = \{n_{nat}(t)\} - \{n_{pert}(t)\}. \tag{26}$$

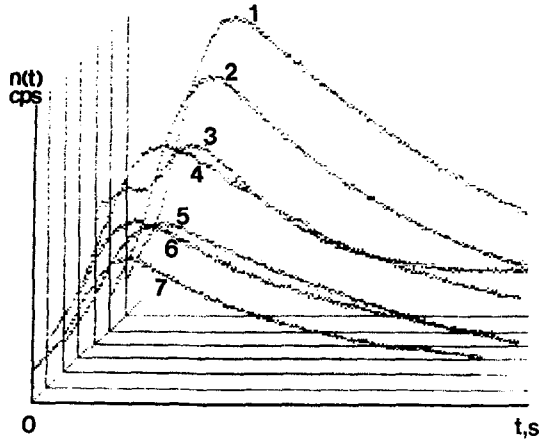

Figure 17. Photon emission processes generated by perturbed human neutrophils stimulated with FMLP. Emission process from unperturbed stimulated neutrophils (1) is non-stationary and has the same form as those from stimulated neutrophils perturbed by DMSO (2), o-xylene (3), p-xylene (4), phenol (5), toluene (6), and benzene (7)[19]. All the processes are shown on the same scale.

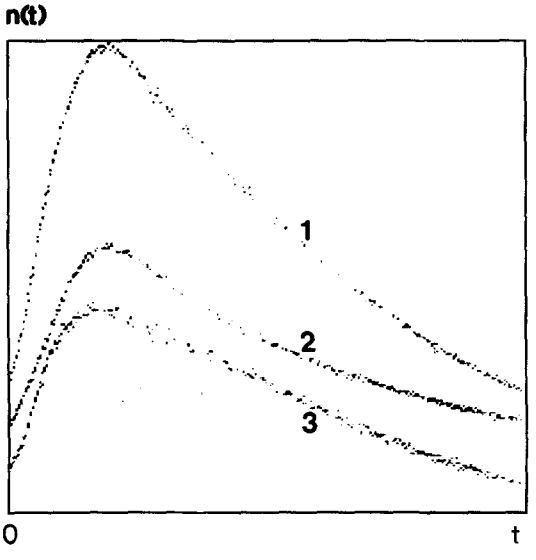

Figure 18. Comparison of the two photon emission processes generated by human neutrophils stimulated (with FMLP), unperturbed (1), and perturbed by toluene (2)[19]. The resulting process $\{n_r(t)\}$ (3) comes into being through comparison of the process $\{n_{pert}(t)\}$ (2) with the process $\{n_{nat}(t)\}$ (1): $\{n_r(t)\} \equiv \{n_{nat}(t)\} - \{n_{pert}(t)\}$; the process (1) in the case of non-stationary emission from native (unperturbed) biosystems is thought to be a reference process just as the process $\{a(t)\}$ was in the instance of stationary uncorrelated emission (see fig. 14).

This trio of processes is shown in figure 18. Descending stages of the processes from figure 18 are presented in figure 19.

From Eq. 26 it is evident that in the absence of perturbation the $\{n_r(t)\}$ process is transformed into white noise with zero mean value. At complete perturbation the resulting process becomes identical to $\{n_{nat}(t)\}$. In consequence the resultant process of any partly perturbed phagocytosis process finds its reference process, i.e. $\{n_{nat}(t)\}$.

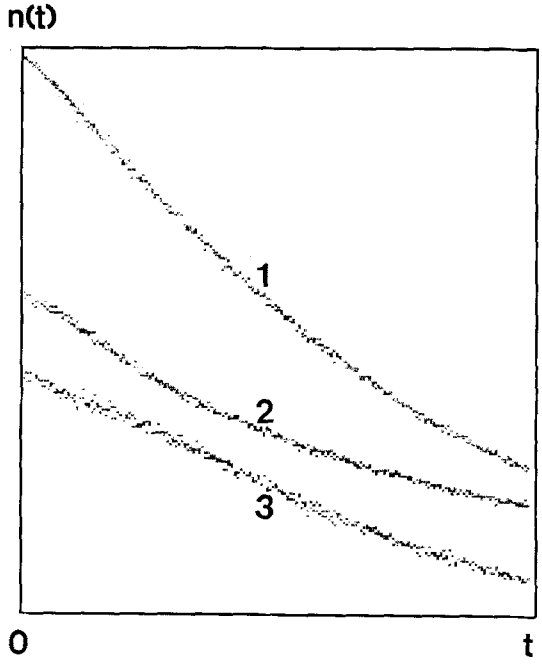

Figure 19. Descending stages of the processes from fig. 18. Resulting processes $\{n_r(t)\}$, such as the one represented by (3), are the basis of construction of new non-local perturbation measures which will hold true when the stationarity of the reference process does not occur and the classical notion of homeostasis is unapplicable.

All the perturbed phagocytosis processes considered here can be described as IMA(0, 1, 1) processes[19]:

$$(1 - B)\,n_r(t) = (1 - \vartheta B)\,a(t) \tag{27}$$

having their ϑ parameters in the range $(\vartheta_{nat}, 1)$, where $\vartheta_{nat} = 0.30 \pm 0.06$ is the parameter corresponding to native phagocytosis.

In general, the parameter $\vartheta_{nat} < 1$ replaces the value $\vartheta = 1$ for stationary uncorrelated emission from unperturbed biosystems which was considered beforehand.

It is interesting to make a short review of the results obtained in Kochel[19].

The perturbation coefficient PC[19] is defined by the equation

$$PC \equiv \frac{1 - \vartheta}{1 - \vartheta_{nat}}\,100[\%]; \tag{28}$$

$PC \in [0, 100]\%$, and its standard deviation are as follows:

$$SD(PC) = \frac{100}{1 - \vartheta_{nat}}\left(SD^2(\vartheta) + \left(\frac{1 - \vartheta}{1 - \vartheta_{nat}}\,SD(\vartheta_{nat})\right)^2\right)^{1/2}, \tag{29}$$

where $SD(\vartheta) = \left(\frac{1 - \vartheta^2}{N - 1}\right)^{1/2}$, N is the number of values in $\{n(t)\}$.

PC has been compared with a 'classical' perturbation coefficient CPC[19]:

$$CPC \equiv \left(1 - \frac{I_{pert}}{I_{nat}}\right)100[\%] \tag{30}$$

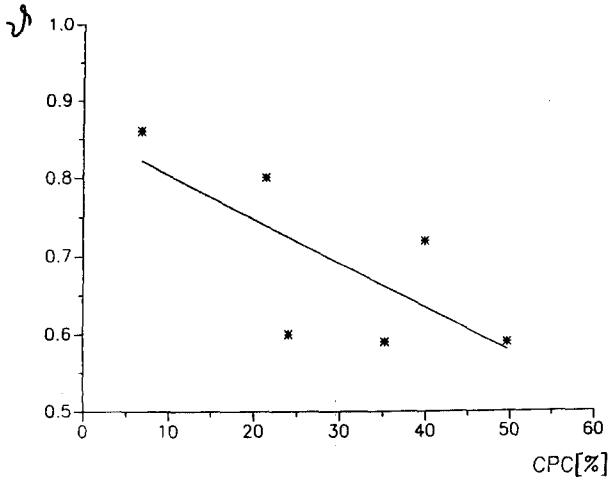

Figure 20. Interdependence between the ϑ parameter and the classical perturbation coefficient CPC for perturbed human neutrophils. Pairs of the ϑ and CPC values have been determined for the resulting processes $\{n_r(t)\}$ corresponding to a variety of used perturbers (see fig. 17). Linear regression $\vartheta(CPC) = 0.725 - 0.002\,CPC$ fits the empirical points with the correlation coefficient -0.37. The large scatter of the CPC values around the regression line, and the result $\vartheta(0) = 0.725$ instead of $\vartheta(0) = 1$, reveal the inadequacy of CPC as a perturbation measure.

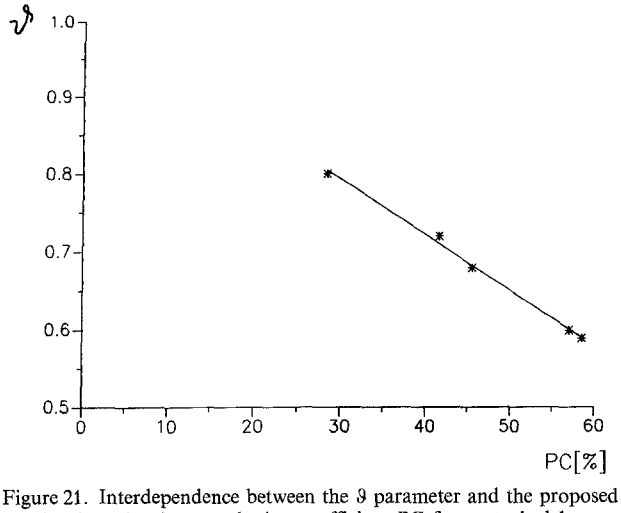

Figure 21. Interdependence between the ϑ parameter and the proposed non-local stochastic perturbation coefficient PC for perturbed human neutrophils; the same samples as in fig. 20. Linear regression $\vartheta(PC) = 1 - 0.007\,PC$ fits the empirical points with correlation coefficient -1.

defined on the basis of the integrated luminescence (I). One can easily see the consistency of PC with T_M and essential divergences between PC and CPC. Those divergences are also seen in figure 20. Of course ϑ as a function of the perturbation magnitude should decrease monotonically, therefore the function $\vartheta = \vartheta(PC)$ should have the same feature. Indeed, $\vartheta(PC) = 1 - 0.007\,PC$ fulfils that condition (fig. 21).

Acknowledgments. The author is indebted to Dr Marek Godlewski, Dr Edward Grabikowski and Mr Waldemar Sajewicz for their cooperation in collecting experimental data.

1 Allen, R. C., Chemiluminescence and the study of phagocyte biochemistry and immunology, in: Biological Luminescence, pp. 429–448. Eds B. Jezowska-Trzebiatowska, B. Kochel, J. Slawinski and W. Strek. World Scientific, Singapore-New Jersey-London-Hong Kong 1990.
2 Bendat, J. S., and Piersol, A. G., Random Data. Analysis and Measurement Procedures. John Wiley & Sons, New York-Chichester-Brisbane-Toronto-Singapore 1986.
3 Bjorn, L. O., Panagopoulos, I., and Bjorn, G. S., Ultraweak luminescence from plant tissue: spectral characteristics and effect of ultraviolet radiation, anaerobiosis and ageing, in: Biological Luminescence, pp. 214–223. Eds B. Jezowska-Trzebiatowska, B. Kochel, J. Slawinski and W. Strek. World Scientific, Singapore-New Jersey-London-Hong Kong 1990.
4 Box, G. E. P., and Jenkins, G. M., Time Series Analysis. Forecasting and Control. Holden-Day, San Francisco 1976.
5 Burr, J. G., Ed., Chemi- and Bioluminescence. M. Dekker, New York 1985.
6 Cannon, W., Bodily Changes in Pain, Hunger, Fear and Rage, W. Norton Co., New York 1929.
7 Cheung, K., Archibald, A. C., and Robinson, M. F., The origin of chemiluminescence produced by neutrophils stimulated by opsonized zymosan. J. Immun. *130* (1983) 2324–2329.
8 Chwirot, W. B., Ultraweak photon emission and another meiotic cycle in *Larix europaea*. Experientia *44* (1988) 594–599.
9 Coleman, B. D., and Noll, W., An approximation theorem for functionals with applications in continuum mechanics. Archs Ration. Mech. Analysis *6* (1960) 355–370.
10 Day, W. A., The Thermodynamics of Simple Materials with Fading Memory. Springer-Verlag, Berlin-Heidelberg-New York 1972.
11 DeChatelet, L. R., Long, G. D., Shirley, P. S., Bass, D. A., Henderson, F. W., and Cohen, M. S., Mechanism of the luminol-dependent chemiluminescence of human neutrophils. J. Immun. *129* (1982) 1589–1593.
12 Guillard, O., and Lauwerys, R., In vitro and in vivo effect of mercury, lead and cadmium on the generation of chemiluminescence by human whole blood. Biochem. Pharmac. *38* (1989) 2819–2823.
13 Gyorkos, J. W., Brock, A. J., and Sparkes, B. G., Chemiluminescence in human whole blood: modulation by the cocarcinogens, phorbol diester and polychlorobiphenyls. Immunopharmac. Immunotoxic. *10* (1988) 417–435.
14 Haldane, J., The Philosophy of a Biologist. Clarendon Press, Oxford 1935.
15 Kochel, B., Grabikowski, E., and Slawinski, J., Analysis of photon-counting time series of low level luminescence from wheat leaves at high temperatures, in: Photon Emission from Biological Systems, pp. 96–109. Eds B. Jezowska-Trzebiatowska, B. Kochel, J. Slawinski and W. Strek. World Scientific, Singapore-New Jersey-Hong Kong 1987.
16 Kochel, B., Slawinski, J., and Grabikowski, E., Nonstationary photon emission from wheat leaves under temperature stress. J. Plant Physiol. *133* (1988) 592–599.
17 Kochel, B., Luminescence of perturbed living organisms: a memory function approach based on linear stochastic models of nonstationary photon emission processes, in: Biological Luminescence, pp. 101–116. Eds B. Jezowska-Trzebiatowska, B. Kochel, J. Slawinski and W. Strek. World Scientific, Singapore-New Jersey-London-Hong Kong 1990.
18 Kochel, B., Perturbed living organisms: a cybernetic approach – founded on photon emission stochastic processes. Kybernetes *19* (1990) 16–25.
19 Kochel, B., A new phagocyte luminescence-based stochastic method for determining cytotoxic effects of xenobiotics, in: Proc. Intern. Conference Human Environment. Eds J. W. Dobrowolski and B. Kochel. Polish Academy of Sciences, European Inst. of Ecology and Cancer, and Intern. Society for Research on Civilization Diseases and on Environment, Wroclaw-Sobotka 1991.
20 Lock, R., and Dahlgren, C., Characteristics of the granulocyte chemiluminescence reaction following an interaction between human – neutrophils and *Salmonella typhimurium* bacteria APMIS *96* (1988) 299–305.
21 Martienssen, W., and Spiller, E., Intensity fluctuations in light beams with several degrees of freedom. Phys. Rev. Lett. *16* (1966) 531.
22 Perina, J., Coherence of Light. Van Nostrand Reinhold, London 1972.
23 Sherstnev, M., Chemiluminescent express-methods in clinical medicine, in: Biological Luminescence, pp. 504–531. Eds B. Jezowska-Trzebiatowska, B. Kochel, J. Slawinski and W. Strek. World Scientific, Singapore-New Jersey-London-Hong Kong 1990.

24 Slawinski, J., and Kochel, B., Stochastic models of nonstationary photon emission from chemically perturbed living organisms, in: Biological Luminescence, pp. 78–100. Eds B. Jezowska-Trzebiatowska, B. Kochel, J. Slawinski and W. Strek. World Scientific, Singapore-New Jersey-London-Hong Kong 1990.
25 Slawinski, J., Ultraweak luminescence and perturbation of biohomeostasis, in: Biological Luminescence, pp. 49–77. Eds B. Jezowska-Trzebiatowska, B. Kochel, J. Slawinski and W. Strek. World Scientific, Singapore-New Jersey-London-Hong Kong 1990.
26 Tilbury, R. N., and Quickenden, T. I., Spectral and time dependence studies of the ultraweak bioluminescence emitted by the bacterium – *Escherichia coli*. Photochem. Photobiol. *47* (1988) 145–150.
27 Tilbury, R. N., Ultraweak luminescence of yeast and bacteria, in: Biological Luminescence, pp. 151–172. Eds B. Jezowska-Trzebiatowska, B. Kochel, J. Slawinski and W. Strek. World Scientific, Singapore-New Jersey-London-Hong Kong 1990.
28 Truesdell, C. A., A First Course in Rational Continuum Mechanics. The Johns Hopkins University, Baltimore 1972.
29 Tryka, S., Ultraweak luminescence from mechanically damaged wheat seeds during imbibition, in: Biological Luminescence, pp. 630–646. Eds B. Jezowska-Trzebiatowska, B. Kochel, J. Slawinski and W. Strek. World Scientific, Singapore-New Jersey-London-Hong Kong 1990.
30 Vysotsky, E. S., Bondar, V. S., Gitelson, I. I., Petrunyaka, V. V., Gamalei, I. A., and Kaulin, A. B., Extraction, some properties and application of obelin, calcium-activated photoprotein, in: Biological Luminescence, pp. 386–395. Eds B. Jezowska-Trzebiatowska, B. Kochel, J. Slawinski and W. Strek. World Scientific, Singapore-New Jersey-London-Hong Kong 1990.
31 Waddington, C. H., ed., Towards a Theoretical Biology, 4 vols. Edinburgh University Press, Edinburgh 1968–1972.
32 Westman, J. A., Influence of pH and temperature on the luminol-dependent chemiluminescence of human polymorphonuclear leukocytes. Scand. J. clin. Lab. Invest. *46* (1986) 427–434.

0014-4754/92/11-12/1059-11$1.50 + 0.20/0

Nonlinear response of biophoton emission to external perturbations

Q. Gu[a, b] and F.-A. Popp[a]

[a]*International Institute of Biophysics, Technology Center, Opelstr. 10, D-6750 Kaiserslautern 25 (Federal Republic of Germany) and* [b]*Department of Physics, Northwest University, Xi'an 710060 (People's Republic of China)*

Abstract. By considering an exciplex system consisting of collective molecules in interaction with both the 'pumping' fields and the biophoton fields, the two-level exciplex model and the three-level exciplex model are presented. They are useful for the investigation of the quasi-stationary behaviour of biophoton emission, and biophoton emission as a dynamic process in the presence of external perturbations. Our theoretical results predict a series of nonlinear effects, such as chaos, fractal behaviour, and non-equilibrium phase transition. These effects characterize the coherence nature of living systems. In our approaches, there are two important quantities f and x, which can be used to mark the working points of the two-level and three-level exciplex systems. All the influences of external perturbations on the exciplex systems, e.g. change of temperature, the addition of agents, exposure to light, etc., can be interpreted as shifts of the working points of the systems, leading to a diversity of nonlinear response of biophoton emission. In addition, the agreements of the theoretical results and the corresponding experimental observations on biophoton emission from biological systems in the presence of external perturbations are demonstrated.
Key words. Exciplex formation; two-level exciplex model; three-level exciplex model; chemical potential; pumping field; collective molecules; chaos; fractal behaviour; non-equilibrium phase transition; working point.

Introduction

'Biophoton emission' is now a topical field in contemporary science[33, 65, 66, 102]. It concerns weak light emission from biological systems, with an intensity of the order of a few up to some hundred photons per second and per square centimeter of surface area.

The origin of biophoton research can be traced back to A. G. Gurwitsch[27, 28, 48]. He performed various experiments on 'mitogenetic radiation' with the aid of biological detectors. Gurwitsch claimed that the most fundamental biological function, namely cell division, is triggered by a very weak photocurrent originating from the cells themselves. Since biological detector systems found little support in the scientific world, and because of the unavailability of sufficiently sensitive technical equipment at that time, no generally accepted conclusion on mitogenetic radiation was reached for quite a long period.

In 1955 Colli et al.[10] succeeded in proving the existence of photon emission from cereals by using a photomultiplier tube. The photons were regarded as visible radiation between 390 and 650 nm with intensities of some hundred photons/(s · cm^2).

In the 1960s most of the research work on biophoton emission was performed by Russian scientists[40, 64, 107, 114], who measured the biophoton emission from about 90 kinds of biological samples, including yeast, frog nerve and mouse liver, again using photomultipliers.

In the last fifteen years, essential progress in this field has been accomplished, involving the following topics: the source of the biophotons[2, 3, 42, 60, 67–69, 86], their correlations with biological, biophysical and biochemical processes[34, 39, 65, 66, 84, 88, 93, 94, 101, 113], the temperature dependence[70, 71, 96, 97], the spectral distribu-